



Cite this: *Polym. Chem.*, 2016, **7**, 6490

Trityl-based alkoxyamines as NMP controllers and spin-labels[†]

Gérard Audran,^a Elena G. Bagryanskaya,^{b,c} Paul Brémond,^a Mariya V. Edeleva,^b Sylvain R. A. Marque,^{*,a,b} Dmitriy A. Parkhomenko,^b Olga Yu. Rogozhnikova,^{b,c} Victor M. Tormyshev,^{b,c} Evgeny V. Tretyakov,^b Dmitry V. Trukhin^{b,c} and Svetlana I. Zhivetyeva^b

Recently, new applications of trityl-nitroxide biradicals were proposed. In the present study, attachment of a trityl radical to alkoxyamines was performed for the first time. The rate constants k_d of C-ON bond homolysis in these alkoxyamines were measured and found to be similar to those for alkoxyamines without a trityl moiety. The electron paramagnetic resonance (EPR) spectra of the products of alkoxyamine homolysis (trityl-TEMPO and trityl-SG1 biradicals) were recorded, and the corresponding exchange interactions were estimated. The decomposition of trityl-alkoxyamines showed more than an 80% yield of biradicals, meaning that the C-ON bond homolysis is the main reaction. The suitability of these labelled initiators/controllers for polymerisation was exemplified by means of a successful nitroxide-mediated polymerisation (NMP) of styrene. Thus, this is the first report of a spin-labelled alkoxyamine suitable for NMP.

Received 27th July 2016,
Accepted 24th September 2016
DOI: 10.1039/c6py01303a
www.rsc.org/polymers

Introduction

Although persistent trityl radicals $\text{Ar}_3\text{C}^\bullet$ were discovered by Gomberg in 1900,¹ only many decades later did these radicals arouse keen interest in the scientific community because of their appealing applications as probes.^{2–4} They are currently used as spin probes for oxymetry,² as pH probes,⁵ and as spin labels for distance measurements in biomolecules.⁶ Very recently, the preparation of nitroxide-trityl radical dual probes was reported⁷ and aroused keen interest, and attracted a lot of attention as probes based on the modulation of the exchange interaction between the two spins⁸ and as polarizing agents for Dynamic Nuclear Polarisation-enhanced Nuclear Magnetic Resonance (DNP-NMR).⁹ In the same period, there was increasing interest in the practical applications of biradicals such as binitroxides because of their uses as an initiator/controller agent in Nitroxide Mediated Polymerization^{10–12} (NMP) and as a polarizing agent in DNP-NMR.¹³

In the last decade, Electron Paramagnetic Resonance (EPR) techniques experienced a tremendous development towards

EPR imaging^{2,14} with the help of new technologies and the preparation of new spin probes such as those mentioned above leading to *in vivo* imaging,¹⁵ and imaging in materials.¹⁶ Moreover, in the last three decades, the chemistry of alkoxyamines $\text{R}_1\text{R}_2\text{NOR}_3$ has been developed for their application to NMP as a controllers/initiators.^{17,18} Lately, new applications of these compounds emerged in materials sciences – as key moieties in self-healing polymers,^{19,20} as fluorescent switches,^{21,22} and as a coding system^{23,24} – as well as in biology as a new type of theranostic agent.²⁵ Taking into account the valuable properties of trityl radicals as spin probes and the possible practical usefulness of alkoxyamines, and their various modes of activation – protonation, oxidation, alkylation, light irradiation – the investigation of the properties of trityl-attached alkoxyamines is a promising field. Here, we report the first preparation of several trityl-alkoxyamines (TA) based on the SG1 and TEMPO nitroxyl fragments (Fig. 1) as well as the homolysis rate constant k_d of the C-ON bond, and the EPR features of the trityl-TEMPO and trityl-SG1 biradicals. Among the family of trityl paramagnets, the Finland-type radical **17** was selected because of the simplicity of its EPR signal (*i.e.* one peak), the suppression of the reactivity at the *para* position by its functionalisation,[‡]²⁶ and due to its carboxylic function suitable for many types of coupling reactions.[§] The trityl

^aAix Marseille Univ, CNRS, ICR, UMR 7273, case 551, Avenue Escadrille Normandie-Niemen, 13397 Marseille Cedex 20, France. E-mail: sylvain.marque@univ-amu.fr

^bN. N. Vorozhtsov Novosibirsk Institute of Organic Chemistry SB RAS, 9, Lavrentjev Avenue, Novosibirsk 630090, Russia

^cNovosibirsk State University, Novosibirsk 630090, Russia

† Electronic supplementary information (ESI) available: EPR simulation data in Table S1; Fig. S1 for decays of 1–5; EPR signal temperature-dependence in Fig. S2 and S3; characterization data in Fig. S4–10. See DOI: 10.1039/c6py01303a

[‡]In ref. 26, the Finland trityl radical **16** is used as a model. Its reactivity with small radicals such as methyl radical Me^\bullet has been reported as extremely low. Consequently, it was assumed unreactive toward the styryl radical due to its size.
[§]Other positions were unreactive due to the substitution by sulphur atoms.



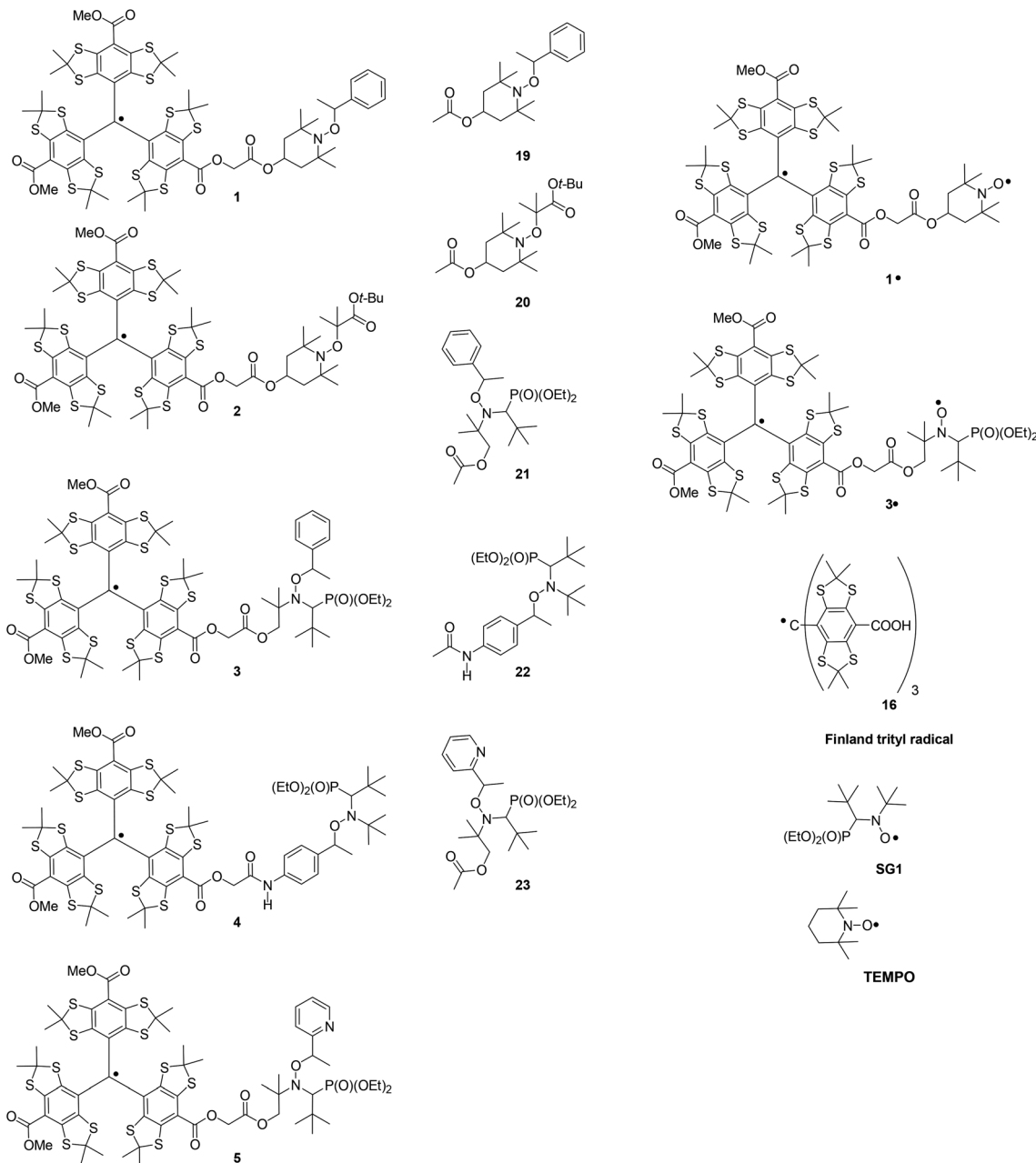


Fig. 1 Trityl-alkoxyamines and the corresponding biradicals under study.

radical was found to have no significant effect on k_d , meaning that these alkoxyamines retained all their kinetic properties for use as a controllers/initiators in NMP, as a switch in optotonics, and as theranostic agents. Moreover, the ability of TA to control NMP was confirmed by the polymerisation of styrene with **1**.

Experimental section

Kinetic experiments

Homolysis rate constants k_d were measured by EPR,²⁷ as previously reported, and given by eqn (1) (Fig. S1†). Air was used

as an alkyl radical scavenger for EPR experiments, respectively. Activation energies E_a were estimated using eqn (2) and the averaged frequency factor $A = 2.4 \times 10^{14} \text{ s}^{-1}$.²⁸ The values of k_d and E_a are listed in Table 1.

$$\ln \frac{[\text{nitroxide}]_\infty - [\text{nitroxide}]_t}{[\text{nitroxide}]_\infty} = -k_d \cdot t \quad (1)$$

$$E_a = 8.314 \cdot T \cdot \ln \frac{2.4 \times 10^{14}}{k_d} \quad (2)$$

Table 1 Experimental homolysis rate constants $k_{d,\text{exp}}$, the corresponding activation energy E_a , and the re-estimated rate constant k_d at 120 °C

TA	Solvent	T (°C)	$k_{d,\text{exp}}^a$ (10^{-4} s $^{-1}$)	E_a^b (kJ mol $^{-1}$)	k_d^c (10^{-4} s $^{-1}$)
1	<i>t</i> -BuPh	125	3.6	135.8	2.1
2	Toluene	80	2.1	122.0	146.0
3	Toluene	100	3.0 ^d	127.8 ^c	24.7
4	Toluene	100	6.0 ^d	125.7 ^c	47.0
5	Toluene	100	6.7 ^d	125.3 ^c	52.4

^a The error on $k_{d,\text{exp}}$ is 5%. ^b Given by eqn (2), with k_d values reported in the 4th column. ^c Re-estimated k_d values at 120 °C using adapted eqn (2) and E_a values reported in the 5th column. ^d A diastereoisomeric mixture.

EPR experiments

The EPR measurements were carried out in CW mode using a Bruker EMX X-band spectrometer equipped with a BVT-2000 temperature control system.¶ The samples were degassed by 3 cycles of a freeze–pump–thaw procedure ($P = 0.1$ mb). The EasySpin software toolbox was used for simulation of the EPR spectra.²⁹ To take into account the presence of various conformers of nitroxide–trityl biradicals showing slightly different spin–spin exchange interaction values, it was assumed that exchange interaction values are prone to a normal distribution with the mean value J and standard deviation ΔJ (eqn (3) and Table S1†).

$$f(x) = \frac{1}{\sqrt{2\pi\Delta J^2}} e^{-\frac{(x-J)^2}{2\Delta J^2}} \quad (3)$$

Polymerization experiments

A weighed amount of **1** (6.5 mg) was dissolved in 3 mL of styrene (distilled prior to the experiment). The reaction mixture was placed in a round-bottom two-neck flask equipped with a magnetic stirrer and a condenser, degassed by Ar bubbling and heated at 130 °C in an oil bath under an inert atmosphere. Sampling was performed by means of a syringe at various time intervals to monitor the evolution of the monomer conversion, molecular weight and PDI of the polymer prepared. The probes were quenched in an ice bath and stored at 4 °C prior to analysis. Monomer conversion was analysed by ¹H NMR. The polymer molecular weight and distribution were analysed by gel permeation chromatography on an Agilent LC 1200 set-up equipped with an isocratic pump, a PL-mixed C GPC column, and UV and refractive index detectors. THF was used as an eluent at a flow rate of 1 mL min $^{-1}$ and the column temperature was set at 35 °C. The column was calibrated by using narrow PDI polystyrene standards (Agilent).

General

Solvents and reactants were used as received. (1-Bromoethyl)benzene (97%), trifluoromethanesulfonate copper(II) ($\text{Cu}(\text{OTf})_2$) (98%) and 4-*tert*-butyl-2-(4-*tert*-butylpyridin-2-yl)pyr-

idine (dTbpy) (98%) were purchased from Aldrich. *tert*-Butyl 2-bromo-2-methylpropanoate was purchased from Fluka. Alkoxyamines **6**,³⁰ **8**,³¹ and **9**³² were prepared according to the literature.^{33,34} 2-Bromoacetyl bromide was obtained by a known literature method.³⁰

Routine reaction monitoring was performed using silica gel 60 F₂₅₄ TLC plates; spots were visualised by exposure to UV light and a phosphomolybdic acid solution in EtOH, followed by heating. Purification procedures were performed on chromatography columns with silica gel grade 60 (230–400 mesh). The ¹H, ¹³C, and ³¹P NMR spectra were recorded with a Bruker AV-400 (¹H: 400.13 MHz, ¹³C{¹H}: 100.61 MHz) and Bruker AV-300 (¹H: 300.13 MHz, ¹³C{¹H}: 75.476 MHz) spectrometer. Deuteriochloroform (CDCl_3) was used as the solvent, with residual CHCl_3 ($\delta_{\text{H}} = 7.25$ ppm) or CDCl_3 ($\delta_{\text{C}} = 77.0$ ppm) being employed as an internal standard. In recording ³¹P-NMR spectra, 85% H_3PO_4 was used as an internal standard ($\delta_{\text{P}} = 0$ ppm). The precise masses of molecular ions were determined by HRMS on a DFS Thermo scientific instrument (EI, 70 eV). The melting point was determined on an FP 900 Thermosystem microscope melting point apparatus (Mettler-Toledo International Inc., Zürich, Switzerland). Elemental analysis was performed on a Euro EA-3000 CHNS analyzer. IR spectra were recorded with a Bruker Tensor 27 FTIR spectrometer, and KBr pellets were used. Wavenumber values are given in cm^{-1} . Electrospray ionization mass spectra ESI/MS were recorded using a hybrid quadrupole/time-of-flight Bruker micrOTOF-Q spectrometer with methanol or dichloromethane (DCM) used as a solvent and scanning the spectra in the m/z range 100–3000 in positive and negative ionization modes. Nitrogen was used as a drying gas at 220 °C and at a flow rate of 4 L min $^{-1}$. The nebulizer pressure was set at 1.0 bar. The capillary voltage was set at –4.0 kV. Sample solutions were infused into the ESI source by using an LC Agilent 1200 in FIA mode (Flow Injection Analysis, 2–3 μ L at a flow rate of the solvent 0.1 mL min $^{-1}$).

General procedure for the preparation of **11–15**

To a stirred solution of alkoxyamine (**6–10**, 0.1 mmol) and pyridine (0.12 mmol) in dry dichloromethane (DCM) (0.25 mL) was added a solution of 2-bromoacetyl bromide (0.13 mmol) in dichloromethane (0.30 mL). The thick caseous solid was immediately obtained, but it disappeared while the mixture was stirred under an argon atmosphere overnight at room

¶ For the characterization of **1–5** under air at 25 °C, recording parameters are: 9.3 GHz; sweep width: 0.2–0.5 mT; microwave power, 1–6 μ W; modulation frequency: 100 kHz; modulation amplitude: 5 μ T; time constant: 81.92–163.84 ms; sweep time: 41.94–83.89 s; number of points: 512; number of scans: 1.



temperature. To the resulting clear solution were added DCM (5 mL) and 0.1 M aqueous HCl (2 mL). The organic phase was separated and filtered through a short plug of silica. The filtrate was concentrated *in vacuo* to yield crude alkoxyamines **11** (68%), **12** (76%), **13** (96%), **14** (92%), and **15** (68%), which were used further without purification.

General procedure for the preparation of 1–5

To an alkoxyamine (**11–15**) were added finely powdered potassium carbonate (10 mg, 0.070 mmol), trityl **17** (50.0 mg, 0.050 mmol), dry acetone (0.300 mL) and anhydrous dimethylformamide (0.15 mL). The heterogeneous mixture was stirred at 40 °C for 24 h under an argon atmosphere, and then diluted with DCM (10 mL) and water (3 mL). The deep-green organic phase was separated, filtered through a short cotton plug and concentrated *in vacuo* to yield a black film. Column chromatography on a silica gel (DCM, then DCM/methanol with a gradual increase in the solvent ratio from 1 : 0.05 to 1 : 0.2 v/v) yielded TA **1–5**, respectively.

Bis[8-(methoxycarbonyl)-2,2,6,6-tetramethylbenzo[1,2-d:4,5-d']bis[1,3]dithiol-4-yl][(8-(2-(4-(1-phenylethoxy)-3,3,5,5-tetramethyl-4-azacyclohexyloxy)-2-oxo-ethyloxy)carbonyl)-2,2,6,6-tetramethylbenzo[1,2-d:4,5-d']bis[1,3]dithiol-4-yl)methyl radical 1. 0.052 g (78%), greenish-black powder, m.p. > 125 °C (decomposition). HRMS (ESI): calcd for $C_{61}H_{70}NO_9S_{12} [M^-]$ 1344.1699, found 1344.167; calcd $C_{61}H_{71}NO_9S_{12} [M + H^+]$ 1345.1777, found 1345.169. IR (KBr): ν = 2953 (m), 2922 (m), 1740 (m), 1707 (vs), 1491 (m), 1452 (m), 1433 (m), 1365 (m), 1306 (m), 1274 (m), 1234 (vs), 1169 (m), 1147 (m), 1134 (s), 1111 (m), 1045 (m), 700 (m). ESR for 0.5 mM deoxygenated solution in DCM: multiplet, α_H = 9.4 μ T, linewidth (Gauss) 8.7 μ T, g = 2.00280.

Bis[8-(methoxycarbonyl)-2,2,6,6-tetramethylbenzo[1,2-d:4,5-d']bis[1,3]dithiol-4-yl][(8-(2-(4-(1-methyl-1-*tert*-butoxycarbonyl-ethyl-oxyl)-3,3,5,5-tetramethyl-4-azacyclohexyloxy)-2-oxo-ethyloxy)carbonyl)-2,2,6,6-tetramethylbenzo[1,2-d:4,5-d']bis[1,3]dithiol-4-yl)methyl radical 2. 0.063 g (91%), black powder, m.p. > 120 °C (decomposition). HRMS (ESI): calcd for $C_{61}H_{76}NO_{11}S_{12} [M^-]$ 1382.2067, found 1382.210; calcd for $C_{61}H_{77}NO_{11}S_{12} [M + H^+]$ 1383.2145, found 1383.217. IR (KBr): ν = 2971 (m), 2953 (m), 2924 (m), 1709 (vs), 1489 (m), 1454 (m), 1435 (m), 1365 (m), 1275 (m), 1234 (vs), 1167 (m), 1134 (s), 1113 (m). ESR for 0.5 mM deoxygenated solution in DCM: multiplet, α_H = 9.4 μ T, linewidth (Gauss) 8.5 μ T, g = 2.00280.

Bis[8-(methoxycarbonyl)-2,2,6,6-tetramethylbenzo[1,2-d:4,5-d']bis[1,3]dithiol-4-yl][(8-(2-(3-(1-phenylethoxy)-4-diethoxyphosphoryl-2,2,5,5-tetramethyl-3-azahexyloxy)-2-oxo-ethyloxy)carbonyl)-2,2,6,6-tetramethylbenzo[1,2-d:4,5-d']bis[1,3]dithiol-4-yl)methyl radical 3. 0.065 g (88%), greenish-black powder, m.p. > 120 °C (decomposition). HRMS (ESI): calcd for $C_{65}H_{81}NO_{12}PS_{12} [M^-]$ 1482.2145, found 1482.251; calcd for $C_{65}H_{82}NO_{12}PS_{12} [M + H^+]$ 1483.2223, found 1483.212; calcd for $C_{65}H_{81}NNaO_{12}PS_{12} [M + Na^+]$ 1505.2043, found 1505.201. IR (KBr): ν = 2968 (m), 2955 (m), 2922 (m), 1709 (s), 1489 (m), 1452 (m), 1435 (m), 1365 (m), 1305 (m), 1272 (m), 1236 (vs), 1169 (m), 1149 (m), 1134 (m), 1111 (m), 1057 (m), 1026 (m), 953 (m). ESR for

0.5 mM deoxygenated solution in DCM: multiplet, α_H = 9.4 μ T, linewidth (Gauss) 8.7 μ T, g = 2.00280.

Bis[8-(methoxycarbonyl)-2,2,6,6-tetramethylbenzo[1,2-d:4,5-d']bis[1,3]dithiol-4-yl][(8-((4-(4-diethoxyphosphoryl-4-*tert*-butyl-1,5,5-trimethyl-3-aza-2-oxahexyloxy)phenylamino)-2-oxo-ethyloxy)carbonyl)-2,2,6,6-tetramethylbenzo[1,2-d:4,5-d']bis[1,3]dithiol-4-yl)methyl radical 4. 0.054 g (73%), deep-green powder, m.p. > 130 °C (decomposition). HRMS (ESI): calcd for $C_{65}H_{83}N_2O_{11}PS_{12} [M + H^+]$ 1482.2383, found 1482.229; calcd for $C_{65}H_{82}N_2NaO_{11}PS_{12} [M + Na^+]$ 1504.2202, found 1504.218. IR (KBr): ν = 2956 (m), 2920 (m), 1709 (s), 1529 (m), 1487 (m), 1452 (m), 1435 (m), 1365 (m), 1271 (m), 1234 (vs), 1167 (m), 1134 (m), 1111 (m), 1053 (m), 1028 (m), 955 (m). ESR for 0.5 mM deoxygenated solution in DCM: multiplet, α_H = 10.6 μ T, linewidth (Gauss) 7.3 μ T, g = 2.00281.

Bis[8-(methoxycarbonyl)-2,2,6,6-tetramethylbenzo[1,2-d:4,5-d']bis[1,3]dithiol-4-yl][(8-(2-(3-(1-(2-pyridyl)ethyloxy)-4-diethoxyphosphoryl-2,2,5,5-tetramethyl-3-azahexyloxy)-2-oxo-ethyloxy)carbonyl)-2,2,6,6-tetramethylbenzo[1,2-d:4,5-d']bis[1,3]dithiol-4-yl)methyl radical 5. 0.032 g (61%), black powder, m.p. > 100 °C (decomposition). HRMS (ESI): calcd for $C_{64}H_{80}N_2O_{12}PS_{12} [M^-]$ 1483.2097, found 1483.178; calcd for $C_{64}H_{81}N_2O_{12}PS_{12} [M + H^+]$ 1484.2176, found 1484.210; calcd for $C_{64}H_{80}N_2NaO_{12}PS_{12} [M + Na^+]$ 1506.1995, found 1506.189. IR (KBr): ν = 2956 (m), 2924 (m), 1745 (s), 1707 (s), 1487 (m), 1452 (m), 1434 (m), 1385 (m), 1365 (m), 1305 (m), 1273 (m), 1236 (vs), 1169 (m), 1149 (m), 1136 (m), 1111 (m), 1055 (m), 1026 (m), 957 (m), 787 (w). ESR for 0.5 mM of 5 in DCM: multiplet (splitting on 8 protons in groups of 3H, 3H, 2H), α_{H1} = 9.0 μ T, α_{H2} = 9.5 μ T, α_{H3} = 9.8 μ T (respectively), linewidth (Gauss) 8.6 μ T, g = 2.00281.

Preparation of *tert*-butyl 2-[(4-hydroxy-2,2,6,6-tetramethylpiperidin-1-yl)oxy]-2-methylpropanoate 7. 0.70 mL (3.7 mmol) of *tert*-butyl 2-bromo-2-methylpropanoate was added to a Schlenk flask with 0.76 g (4.4 mmol) of 4-hydroxy-TEMPO, 0.24 g (3.9 mmol) of copper powder, 0.013 g (0.037 mmol) of $Cu(OTf)_2$ and 0.040 g (0.15 mmol) of dTbpy. Benzene, 5 mL, was then added as a solvent, and the solution was degassed by three freeze-pump-thaw cycles. The solution was heated to 75 °C with stirring. After 5 h, all the copper powder was consumed and a beige precipitate was formed. The solution was filtered and concentrated under vacuum. The crude product was purified by column chromatography eluting with hexane/ethyl acetate (95/5 gradually increasing to 5/5). The alkoxyamine was eluted before 4-hydroxy-TEMPO and collected as a colorless fraction. After evaporation of the solvent, the dry residue was recrystallized from hexane to give 0.97 g (83%) of compound 7 as white crystals, mp 83.8 °C followed by decomposition. 1H NMR (400.13 MHz, $CDCl_3$) δ : 4.00–3.90 (m, 1H), 1.82 (dm, 2H, J_d = 12.2 Hz), 1.46 (s, 10H), 1.41 (s, 7H), 1.20 (s, 7H), 1.07 (s, 6H). $^{13}C\{^1H\}$ NMR (100.61 MHz, $CDCl_3$) δ : 173.9, 80.2, 79.3, 61.6, 58.8, 47.8, 32.3, 26.7, 23.3, 20.1. IR (neat): 3491 m, 3280 w, 3003 m, 2978 s, 2943 m, 2897 m, 1716 s, 1693 s, 1475 m, 1460 m, 1452 m, 1392 w, 1371 s, 1336 w, 1313 m, 1298 m, 1259 m, 1248 m, 1209 m, 1178 m, 1157 s, 1140 vs, 1080 w, 1047 s, 1034 w, 1020 w, 1009 vw, 958 m, 943



w, 930 w, 901 w, 847 m, 818 w, 773 w, 746 w, 590 w, 561 w, 542 w, 500 w, 480 vw cm^{-1} ; HRMS: calcd for $\text{C}_{17}\text{H}_{33}\text{NO}_4$ [M] 315.2404; found 315.2408; Anal. calcd for $\text{C}_{17}\text{H}_{33}\text{NO}_4$: C, 64.73; H, 10.54; N, 4.44. Found: C, 64.95; H, 10.56; N, 4.62.

Bis[8-(methoxycarbonyl)-2,2,6,6-tetramethylbenzo[1,2-*d*:4,5-*d*']bis[1,3]dithiol-4-yl](8-carboxyl-2,2,6,6-tetramethylbenzo[1,2-*d*:4,5-*d*']bis[1,3]dithiol-4-yl)methyl radical 17.³⁶ To a stirred solution of tris[(8-carboxy)-2,2,6,6-tetramethylbenzo[1,2-*d*:4,5-*d*']bis[1,3]dithiol-4-yl]methanol **24**³⁵ (1.018 g, 1.00 mmol) and triethylamine (0.404 g, 4.00 mmol) in methanol (2.5 mL) was added a solution of freshly distilled methyl iodide (0.850 g, 6.00 mmol) in DCM (2.5 mL). The resulting mixture was stirred under an argon atmosphere at 40 °C for 36 h. 0.5 M aqueous HCl (4 mL) and DCM (5 mL) were added. The organic layer was separated, and the water phase was extracted with DCM (3 × 5 mL). The combined organic extract was washed with brine, filtered through a short silica plug, concentrated *in vacuo*, and dried in a desiccator to quantitatively yield triarylmethanol **25** (1.052 g). Hydrolysis of **25** into monocarboxylic acid **26** and further conversion of the diamagnetic intermediate **26** into trityl **17** were performed as reported.³⁶ Spectroscopy data for diamagnetic substrates **25** and **26** (¹H-NMR, ¹³C-NMR, FTIR and ESI-HRMS) and trityl **17** (FTIR, ESI-HRMS and ESR) are in agreement with the literature data.³⁶

Results and discussion

Preparation of 1–5

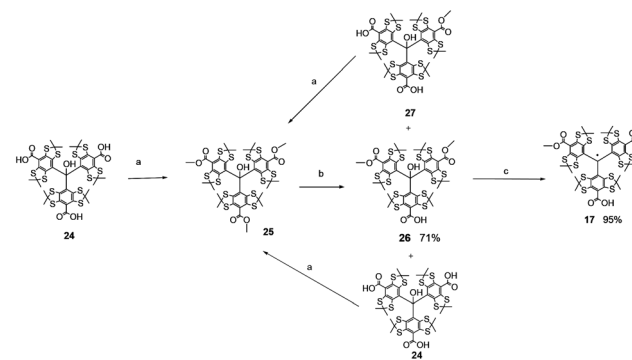
Quantitative methylation of **24**³⁵ yielded **25** which was smoothly hydrolysed under controlled conditions|| into monoacid **26**. The latter, in the presence of a strong acid, afforded its cation derivative which was reduced to trityl **17** in the presence of tin chloride (Scheme 1).³⁶ The trityl radical **17** was used for this purpose because the H-couplings of the odd electron are efficiently suppressed *via* the substitution of the *ortho*, *meta* and *para* hydrogen atoms by sulphur-centred and carbon centred substituents.

Thus, trityl-alkoxyamines **1–5** were prepared in two steps starting from the initial alkoxyamines **6–10**, respectively, and using bromo acetyl bromide as an acetylating agent and a precursor of a spacer, and trityl radical **17** as a monofunctional nucleophile (Scheme 2). Alkoxyamine-trityl radicals **1**, and **3–5** were prepared from the diastereoisomeric mixtures of **6**, and **8–10**, respectively. Trityl-alkoxyamines **1–5** were identified by EPR, IR, and HRMS.

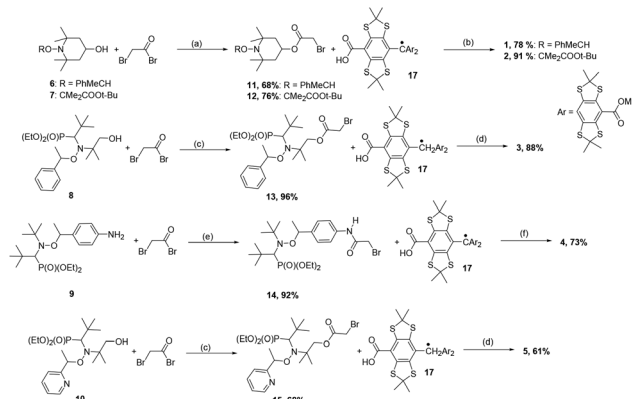
Homolysis of the C-ON bond of alkoxyamines

Rate constants k_d were measured by EPR because the generated nitroxides are stable under our conditions (Table 1). As discussed in the later section, a spin–spin exchange inter-

|| Hydrolysis of **25** is not selective and the dicarboxylic acid **27** and the tricarboxylic acid **24** are generated. Both are re-methylated to yield **25**, and are again smoothly hydrolysed. After three cycles, triarylmethanol **26** was obtained in 71% yield.



Scheme 1 Synthesis of trityl **17**. (a) Methyl iodide (6 equiv.), triethylamine (4 equiv.), 40 °C, 36 h; (b) LiOH (1.55 equiv.) in THF/water, room temperature, 48 h; (c) $\text{CF}_3\text{SO}_3\text{H}$ (5 equiv.) in anhydrous DCM and treated with SnCl_2 (1 equiv.).



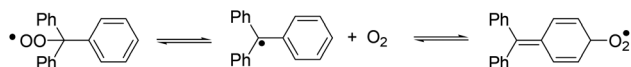
Scheme 2 Preparation of **1–5**. (a) Pyridine (1.2 equiv.) in DCM, room temperature, 24 h; (b) K_2CO_3 in anhydrous acetone/dimethylformamide, 40 °C, 24 h, under an argon atmosphere; (c) pyridine (1.2 equiv.) in dichloromethane, room temperature, 24 h; (d) K_2CO_3 in anhydrous acetone/dimethylformamide, 40 °C, 24 h under argon; (e) pyridine (1.2 equiv.) in dichloromethane, room temperature, 24 h; (f) K_2CO_3 in anhydrous acetone/DMF, 40 °C, 24 h, under an argon atmosphere.

action is observed between the odd electrons localised on the trityl and nitroxyl radical moieties. Nevertheless, the occurrence of this interaction does not impede the determination of k_d by EPR. Gomberg's radical and some other trityl radicals are known to react slowly in a reversible manner with oxygen as displayed in Scheme 3. Because of its functionalisation at the *para* position, the occurrence of the reactivity displayed in Scheme 3 is expected to be very low in the Finland-type trityl radical **17**.^{**}

The homolysis rate constants k_d for the C-ON bond in alkoxyamines are easily estimated using robust linear free energy relationships developed for nitroxyl (eqn (4))³⁷ and

** In this case, the main coupling reaction is expected to occur at the carbonyl centre, which is severely sterically hindered, and consequently, shows negligible reactivity.



Scheme 3 Reactivity of O_2 with Gomberg's radical.

alkyl (eqn (5))^{††}³² fragments in alkoxyamines. Although long-range polar and steric effects are observed in alkoxyamines, for the sake of simplicity, it was assumed that the trityl group is far enough from the reactive centre so that it does not play any role in the bulkiness and polarity of both the nitroxyl and alkyl fragments. Consequently, it was assumed that alkoxyamines **19–23** are suitable models for estimation of the k_d values for **1–5**, respectively, using eqn (4) and (5). The effects of the bulkiness and polarity of the substituents attached to the nitroxyl moiety are estimated using the steric constant E_s ^{37–39} and the localised electrical Hammett constant σ_I .⁴⁰

The polarity effect of the substituent at the *para* position in the aromatic ring is described by the localised electrical Hammett constants $\sigma_{I,p-X-C_6H_4}$.^{41,42} Thus, k_d values were estimated at 120 °C as $2.9 \times 10^{-4} \text{ s}^{-1}$, $1.5 \times 10^{-3} \text{ s}^{-1}$, and $3.3 \times 10^{-3} \text{ s}^{-1}$ for **19** ($E_a = 134.8 \text{ kJ mol}^{-1}$, eqn (4)),^{††} **21** ($E_a = 129.4 \text{ kJ mol}^{-1}$, eqn (4)),^{††} **22** ($E_a = 126.9 \text{ kJ mol}^{-1}$, eqn (5)), respectively. Although no relationships are available to estimate E_a for **20**, the model of **2**, the substituent scale developed a decade ago⁴⁴ provides a difference in E_a , $\Delta E_a = -12.8 \text{ kJ mol}^{-1}$ from the CHMePh group to the CMe₂COOR group affording $E_a = 122.8 \text{ kJ mol}^{-1}$ for **20**. Although no relationships are available to estimate the E_a of **23**, the model of **5**, the replacement of styryl alkyl fragments by a pyridyl fragment is known to decrease the E_a by *ca.* 3 kJ mol⁻¹ in SG1-based alkoxyamines.^{45,46} Thus, because the nitroxyl fragment is the same for **23** and **21**, the E_a for **23** is expected to be *ca.* 3 kJ mol⁻¹ lower than the E_a for **21**, *i.e.* $E_a \approx 126.5 \text{ kJ mol}^{-1}$ and $k_d = 3.7 \times 10^{-3} \text{ s}^{-1}$.

$$\log(k_d/\text{s}^{-1}) = -5.81(\pm 0.09) - 2.91(\pm 0.13) \cdot \sigma_I - 0.85(\pm 0.03) \cdot E_s \quad (4)$$

†† This relationship was specifically developed for the SG1 moiety carrying a *para*-substituted aryl fragment.

‡‡ Steric constant E_s is a linear combination of the steric demand $r_{(i)}$ of each group attached to the nitroxyl moiety (see ref. 37 and 38). Some years ago, constants for cyclic nitroxyl fragments have been developed (ref. 39), and it is assumed that $r_{(\text{Me}_3\text{CH}_2\text{CHOAcCH}_2\text{CMe}_2)} = r_{(\text{R}_2\text{CCH}_2\text{CHOCH}_2\text{CR}_2)} = 0.22$, $r_{(\text{Me})} = 0.00$, and $E_s = -2.70$. The electrical effect is accounted by the sum of the electrical effect of each group attached to the nitroxyl moiety (ref. 37), $\sigma_{\text{I,Me}} = -0.01$, $\sigma_{\text{I,CH}_2\text{CHOAcCH}_2} = 2 \times (\sigma_{\text{I,CH}_2\text{CHOAcMe}}/2) = \sigma_{\text{I,CH}_2\text{CHOAcMe}} \approx \sigma_{\text{I,CH}_2\text{CHOAcMe}} = 0.05$ (see ref. 39 and 40) and $\sigma_I = 0.01$.

§§ Recently, we showed that the leveled steric effect (see ref. 43) applies to this family of molecules. Thus, for instance, the same steric demand is assumed for the CH_2OAc group as for the COOMe group, *i.e.* $E_s = -5.0$ as given in ref. 37. The electrical effect is described by the sum of the electrical effect of each group attached to the nitroxyl moiety (ref. 37 and 40), $\sigma_{\text{I,H}} = 0.00$, $\sigma_{\text{I,Me}} = \sigma_{\text{I,t-Bu}} = -0.01$, $\sigma_{\text{I,P(O)(OEt)}} = 0.32$, $\sigma_{\text{I,CH}_2\text{OAc}} = 0.15$, and $\sigma_I = 0.43$.

¶¶ $\sigma_{I,p-X-C_6H_4}$ is a linear combination of the electrical localized Hammett constant $\sigma_{I,X}$ and of the delocalized Hammett constant $\sigma_{R,X}^0$ (see ref. 40 and 41). $\sigma_{\text{I,NHAc}} = 0.28$, $\sigma_{\text{I,NHAc}}^0 = -0.25$ and $\sigma_{I,p-X-C_6H_4} = -0.08$.

$$\log(k_d/\text{s}^{-1}) = -3.1(\pm 0.1) - 7.8(\pm 0.4) \cdot \sigma_{I,p-X-C_6H_4} \quad (5)$$

The E_a and k_d values predicted by the simplified models **19–23** are in very good agreement with the experimental values reported in Table 1 for **1–5** highlighting both the validity of our assumptions and the robustness of the linear free energy relationship developed (eqn (4) and (5)), *i.e.* k_d values differ by less than 40% and E_a less than 1.7 kJ mol⁻¹. Moreover, as reported for other bisnitroxides,^{12,47,48} the spin–exchange interaction (*vide supra*) has no significant influence on the C–ON bond homolysis.

EPR analysis of **1**· and **3**·

Before heating, the samples of **2** and **3** displayed only the signal of the pure trityl radical as expected (not shown). Upon heating at 100 °C for 5 hours,||| in toluene in the presence of oxygen as an alkyl radical scavenger, for both **2** and **3**, the EPR signal that was recorded at room temperature was due to three species. Considering the experimental conditions, the presence of starting materials was discarded, and the EPR signals were simulated using three new species, namely biradical **1**· or **3**·, free trityl radical and free nitroxides TEMPO or SG1.

Although the trityl and nitroxyl radical moieties are separated by a linker of nine and eight single bonds for **1**· and **3**·, respectively, spin–spin exchange interactions are expected to occur both in **1**· and **3**· due to the freedom of motion of the linker. Therefore, the value of the exchange interaction J was selected as one of the simulation parameters, *i.e.*, J is 63 G and 170 G for **1**· and **3**·, respectively. The accurate simulation of the EPR spectra implies the finding of all stable conformers of **1**· and **3**· with the corresponding J values and implements chemical exchange between all these conformers, but it is a rather complicated task. For simplicity, it is assumed that the values of spin–spin exchange interactions are subject to a normal (Gaussian) distribution with standard deviation ΔJ . The temperature dependence of the signal (Fig. S2†) showed an increase in the spin–spin exchange interaction both for **1**· and **3**· with increasing temperature due to an increase in the mobility of **1**· and **3**·. A very good agreement (Fig. 2a) was achieved and the EPR hyperfine coupling constants (J value between 50 and 100 G) of **1**· are in agreement with those reported in the literature and do not deserve more comments.⁴⁹ On the other hand, as far as we know, the EPR signal of **3**· (Fig. 2b) is the first report of a biradical combining trityl and β -phosphorylated nitroxide. The simulations afforded 14% TEMPO, 6% free trityl, and 80% **1**· for the decomposition of **2**, and 8% SG1, 4% trityl, and 88% **3**· for the decomposition of **3**. Even though more than 80% of released biradicals are observed,*** the detection of

||| After this time of heating, the concentrations in **2** and **3** are estimated, from the data reported in Table 1, as $2 \times 10^{-20} \text{ M}$ and $5 \times 10^{-7} \text{ M}$, respectively.

*** The less than 20% loss is mainly due to the errors in the preparation of the samples (small amounts) and in the reference (TEMPO) used to estimate the radical concentration. Moreover, side-reactions are also possible as mentioned in the article.



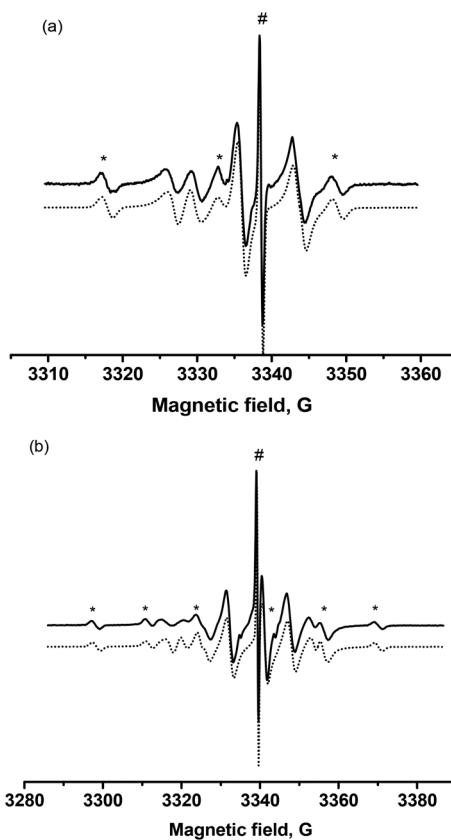
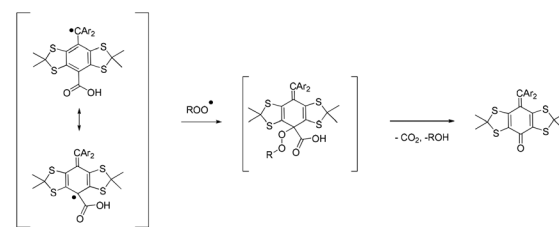


Fig. 2 EPR spectrum of the solution of (a) 1^* and (b) 3^* after 6 hours of heating of a 0.1 mM solution of **2** and **3** at 100 °C in toluene in oxygen saturated solution. (*) Free nitroxide, (#) free trityl radical, a solid line for the experimental spectrum, and a dotted line for the simulated spectrum. Parameters of simulation: (a) $J = 63$ G, $\Delta J = 30$ G for 1^* , and TEMPO: $a_N = 15.4$ G, $g = 2.00595$; (b) $J = 170$ G, $\Delta J = 130$ G for 3^* , and SG1: $a_N = 13.6$ G, $a_P = 44.9$ G and $g = 2.00595$. For a trityl radical: $g = 2.00281$.

free nitroxides and free trityl points to the occurrence of side-reactions.†††

Under the experimental conditions (100 °C in toluene with non-reversible scavenging by O_2 of the generated alkyl radicals, $k_1 \approx 10^9 M^{-1} s^{-1}$),⁵⁰ the homolysis of the alkoxyamines ('T-N-R') is expected to produce only the signal of the biradicals ('T-N * ') 1^* and 3^* (Scheme 5). Accordingly, the presence of free trityl and free nitroxides denotes the occurrence of side-reactions although they occur to a low extent and do not impede the determination of k_d . Furthermore, to take into account these side-reactions, a 10-reaction scheme is proposed with alkoxy and peroxy radicals as reactive key intermediates (Scheme 5). Importantly, several species are expected to provide the same signal, that is the signal of the free nitroxide is due to N^* , X_1N^* , X_2N^* , and X_3N^* , and the signal of the free trityl radical is due

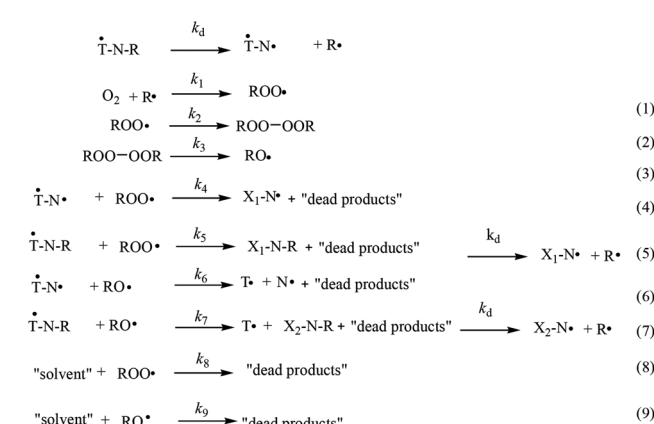
†††Unfortunately, we did not succeed in the experimental measurements of the generation kinetics for individual species (trityl, nitroxide, biradical) due to the complexity of the EPR spectrum, *e.g.* broadening of the spectral lines in the presence of oxygen dissolved in toluene and their consecutive overlapping.



Scheme 4 Conversion of trityl carboxylic acids to diamagnetic species in oxidative reactions with alkylperoxyl radicals.

to only T^* as the starting materials 'TNR' decomposed completely.

Although the *para*-positions on the aromatic rings of trityl radicals of type **17** are substituted by carboxylic acids or carboxylates, reaction with peroxy radicals has been reported at the *para* position (Scheme 4), and is considered one of the main pathways of trityl radical decay.^{51–53} Consequently, the analogous reaction with trityl radicals carrying ester groups cannot be disregarded and might account for the decay of the trityl signal. It is noteworthy that in the case of the 'TN' biradical and 'TNR' alkoxyamine, the reaction with the alkylperoxyl radical would afford a free nitroxide X_1N^* (Scheme 5). For the sake of simplicity, it is assumed that the peroxy radicals reacted in the same way and with the same rate constants with 'TNR' and 'TN', that is $k_4 = k_5 \approx 10^6 M^{-1} s^{-1}$.⁵⁴ The dimerization of peroxy radicals into tetroxides $ROOOOR$ ($k_2 \approx 10^3$ – $10^6 M^{-1} s^{-1}$),^{54,55} which spontaneously and instantaneously collapse into alkoxy radicals ($k_3 > 10^4 s^{-1}$),⁵⁴ is well known and may result in unexpected chemistry.⁵⁶ Therefore, reactions (6) and (7) (Scheme 5) involving alkoxy radicals are included in the kinetic scheme to account for the generation of free trityl radicals. The reactivity is expected to take place in the linker *via* an H-abstraction reaction affording an alkyl radical which then decomposes into a free trityl radical and a nitroxide or alkoxyamine. For simplicity, it is assumed that the alkoxy radicals reacted in the same way and with the same



Scheme 5 The reaction scheme describing decomposition of alkoxyamines **1**–**5** in the presence of oxygen, and applied to account for the EPR signal reported in Fig. 2.



rate constants with 'TNR' and 'TN', that is $k_6 = k_7 > 10^6 \text{ M}^{-1} \text{ s}^{-1}$.^{54,57} For simplicity, as the reaction with the trityl moiety and the linker takes place far from the C-ON bond, it is assumed that the new alkoxyamines generated $\mathbf{X}_1\mathbf{NR}$, and $\mathbf{X}_2\mathbf{NR}$ are homolysed at the same rate as the starting material 'TNR'. The same reactions with the peroxy radicals are disregarded because the H-abstraction rate constants are expected to be low.⁵⁵ Reactions (8) and (9) (Scheme 5) are expected to account for the decay of alkoxy and peroxy radicals in non-reactive by-products. These reactions describe a complicated scheme of decays involving several reactions. For the sake of simplicity, pseudo-first order decays and similar rate constants for the alkoxy and peroxy radicals, *i.e.*, $k_8 = k_9 = 1000 \text{ s}^{-1}$ (this rate was modulated to reach the best simulation) are assumed. Under these experimental conditions, nitroxides are known to be stable in the presence of oxygen, and thus we can assume that the nitroxyl moiety of the generated biradical doesn't take part in any other reactions.

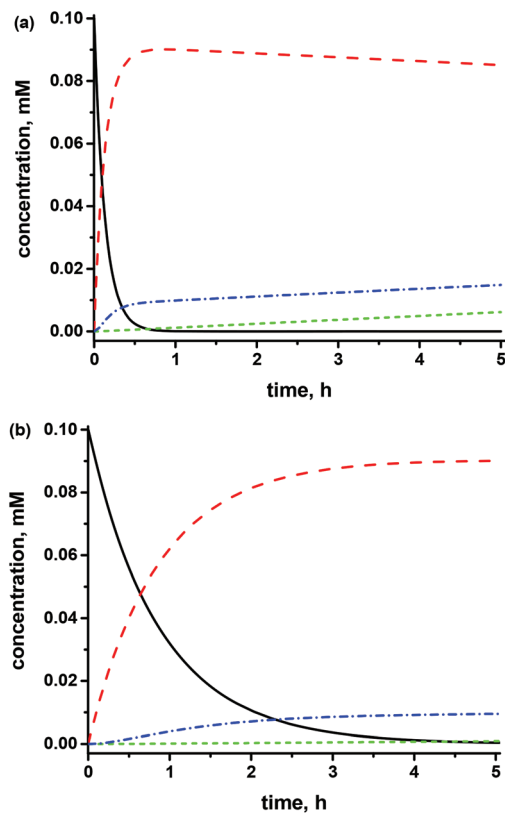


Fig. 3 Time dependence of the concentrations of **2** (a) and **3** (b), bi-radical **1**· (a) and **3**· (b), trityl and free nitroxides TEMPO (a) and SG1 (b) after the thermal decomposition of alkoxyamines as given in Scheme 5. Kinetics parameters: $k_1 = 10^9 \text{ M}^{-1} \text{ s}^{-1}$, $k_2 = 10^4 \text{ M}^{-1} \text{ s}^{-1}$, $k_3 = 10^4 \text{ s}^{-1}$, $k_4 = k_5 = 10^6 \text{ M}^{-1} \text{ s}^{-1}$, $k_6 = k_7 = 3 \times 10^6 \text{ M}^{-1} \text{ s}^{-1}$, $k_8 = k_9 = 1000 \text{ s}^{-1}$, and $[\text{O}_2]_0 = 8 \text{ mM}$. (a) $[\mathbf{2}]_0 = 10^{-4} \text{ M}$ and $k_d = 2 \times 10^{-3} \text{ s}^{-1}$; (b) $[\mathbf{3}]_0 = 10^{-4} \text{ M}$, $k_2 = 10^7 \text{ M}^{-1} \text{ s}^{-1}$, $k_8 = 1000 \text{ s}^{-1}$, $k_9 = 10^6 \text{ s}^{-1}$ and $k_d = 3 \times 10^{-4} \text{ s}^{-1}$. A dashed red line for trityl-nitroxides, a black solid line for TA, a dotted green line for the free trityl radical, and a dashed/dotted blue line for free nitroxides.

Using a reasonable set of rate constants for Scheme 5, it is possible to reach a good agreement, *i.e.*, 14% TEMPO, 6% trityl, and 80% **1**· in radical species, with the ratios reported in Fig. 3a. Nevertheless, these side-reactions do not impede the use of **1**–**5** as initiators/controllers in NMP or the use of their corresponding biradicals (or trityl radical) as probes as long as TA is not overheated for a long period. At the same parameters (Fig. 3b) 10% SG1, 1% trityl, and 89% **1**· after 5 h are obtained, in good agreement with the EPR analysis (Fig. 2b).

Polymerization of styrene initiated with **1**

The possible usefulness of **1**–**5** as initiators in nitroxide mediated polymerization is highlighted by the successful controlled bulk polymerization of styrene with **1** as an initiator/controller (Fig. 4) with styrene/**1** ratios of 5000 : 1 and 1350 : 1, according to the linear increase in molecular weight with conversion upon polymerisation of styrene. The polydispersity index (PDI, Fig. 4) decreases with the conversion as expected and is close to 1.5, *i.e.* slightly larger for the high ratio (targeted M_n of 500 000 g mol⁻¹), due to the occurrence of self-initiation,⁵⁸ and lower for the small ratio (targeted M_n of 135 000 g mol⁻¹).

To check the "living" character of the polymerization, end group analysis is performed. The polymer was precipitated

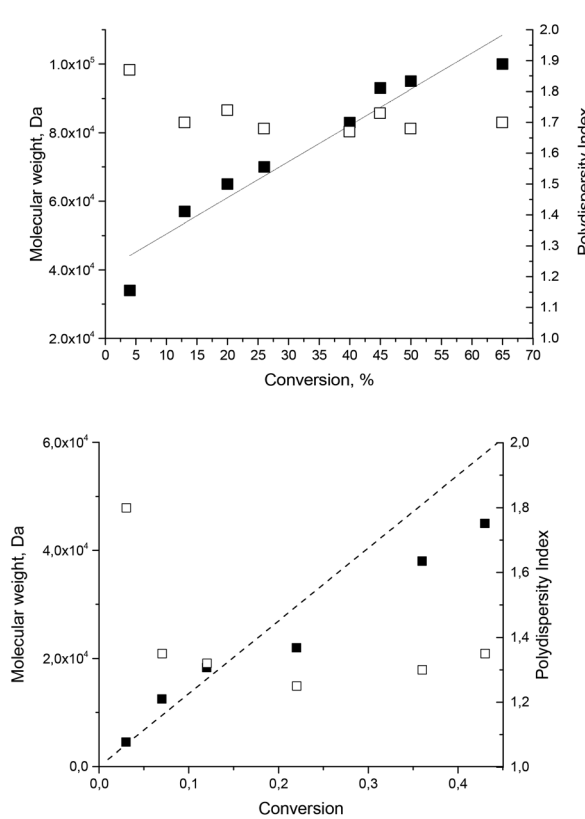


Fig. 4 Molecular weight (left axis, filled squares) and polydispersity index (right axis, open squares) evolution vs. conversion plot for bulk polymerization of styrene initiated with alkoxyamine **1** at 130 °C (top) and 125 °C (bottom) with styrene/**1** ratios 5000 : 1 (top) and 1350 : 1 (bottom). A dotted line for the theoretical evolution of M_n .

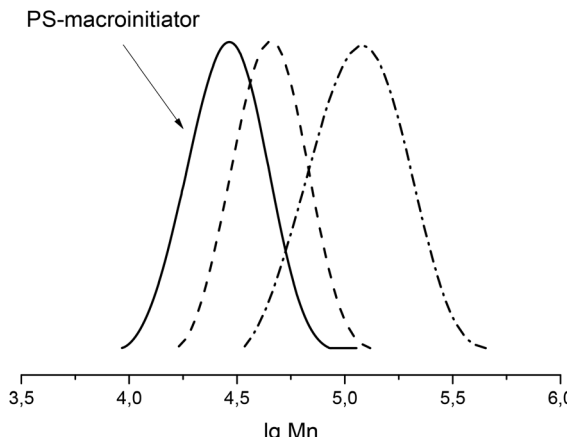


Fig. 5 Re-initiation test in bulk styrene at 125 °C using a PS-macroinitiator ($M_n = 43\,000\text{ g mol}^{-1}$) based on **1** with a styrene/initiator ratio of 2000 : 1. Sampling at 90 minutes and 4 hours.

from the reaction mixture, washed and dried. After that the polymer was dissolved in toluene (10^{-4} M solution based on the molecular weight). EPR is recorded to determine the concentration of the spin labels. The signal of the trityl radical ($9 \times 10^{-5}\text{ M}$ concentration) is observed as expected. The solution saturated with oxygen is heated at 120 °C for 5 hours. Subsequent EPR showed the formation of biradical **1**· with the double integration of the signal twice the one of the starting materials **1** as expected, meaning the decomposition of polymeric alkoxyamines occurred and proving the presence of a nitroxyl end group in the polymer. The fraction of “living” chains is estimated as 90%. The EPR spectra of the polymer sample before and after heating are displayed in Fig. S11.†

Re-initiation of the radical polymerization of bulk styrene (Fig. 5) using a polystyrene macro-initiator based on **1** confirmed nicely the reported livingness.

Taking into account the data reported in the literature, as good as livingness and controlled polymerization are expected with TA 2–5.^{18,28,59,60}

Conclusion

A convenient two-step preparation of the first trityl-alkoxyamines is reported. The observed homolysis rate constants, k_d , for trityl-alkoxyamines are similar to those for the corresponding unlabelled alkoxyamines. It is clearly shown that the trityl radical moiety has no influence on k_d regardless of its position, *i.e.* in the alkyl fragment for **4** or in the nitroxyl fragment for **1–3** and **5** which can be externally activated on the pyridyl moiety. The preservation of the kinetic properties of the alkoxyamines opens up many opportunities for practical applications in polymer sciences, materials sciences, and in theranostics. For example, we can envision the use of trityl as an end-group to track the distribution of polymer drugs, or it may be used to dope the magnetic properties of some materials.

Acknowledgements

Alkoxyamine **10** was kindly provided by Dr J.-P. Joly. GA, PB, and SRAM thank Aix-Marseille Université, CNRS, ANR (ANR-14-CE16-0023-01) and the A*MIDEX project (ANR-11-IDEX-0001-02) funded by the “Investissements d’Avenir” French Government program, managed by the French National Research Agency (ANR), the Fondation ARC pour la recherche sur le cancer (PJA 20141201886). EGB, MVE, SRAM, DAP, EVT, VMT and SIZ are grateful to the Russian Science Foundation (15-13-20020) for financial support. The authors thank Andrey Kuzhelev for recording and simulation of the EPR spectra of compounds **1–5**. NMR, high-resolution ESI/MS, and ESR experiments were carried out in the Chemical Service Center of the Siberian Branch of the RAS.

Notes and references

- 1 M. Gomberg, *J. Am. Chem. Soc.*, 1900, **22**, 757.
- 2 B. Epel, G. Redler, C. Pelizzari, V. M. Tormyshev and H. J. Halpern, Approaching Oxygen-Guided Intensity-Modulated Radiation Therapy, *Oxygen Transport to Tissue XXXVII, V.876 of the series Advances in Experimental Medicine and Biology, Part IV*, 2015, p. 185.
- 3 E. G. Bagryanskaya, E. G. Krumkacheva, M. V. Fedin and S. R. A. Marque, *Methods Enzymol.*, 2015, **563**, 365.
- 4 I. Marin-Montesinos, J. C. Paniagua, A. Peman, M. Vilaseca, F. Luis, S. Van Doorslaer and M. Pons, *Phys. Chem. Chem. Phys.*, 2016, **18**, 3151.
- 5 I. Dhimitruka, A. A. Bobko, C. M. Hadad, J. L. Zweier and V. V. Kramtsov, *J. Am. Chem. Soc.*, 2008, **130**, 10780.
- 6 G. Y. Shevelev, O. A. Krumkacheva, A. A. Lomzov, A. A. Kuzhelev, O. Y. Rogozhnikova, D. V. Trukhin, T. I. Troitskaya, V. M. Tormyshev, M. V. Fedin, D. V. Pyshnyi and E. G. Bagryanskaya, *J. Am. Chem. Soc.*, 2014, **136**, 9874.
- 7 Y. Liu, F. A. Villamena, Y. Song, J. Sun, A. Rockenbauer and J. L. Zweier, *J. Org. Chem.*, 2010, **75**, 7796.
- 8 X. Tan, Y. Song, H. Liu, Q. Zhong, A. Rockenbauer, F. A. Villamena, J. L. Zweier and Y. Liu, *Org. Biomol. Chem.*, 2016, **14**, 1694.
- 9 G. Mathies, M. A. Caporini, V. K. Michaelis and Y. Liu, *Angew. Chem., Int. Ed.*, 2015, **54**, 11770.
- 10 E. Yoshida and K. Takeda, *Polym. J.*, 2001, **33**, 590.
- 11 N. L. Hill and R. Braslau, *Macromolecules*, 2005, **38**, 9066.
- 12 A. Kaim, K. Pietrasik and T. Stokłosa, *Eur. Polym. J.*, 2010, **46**, 519.
- 13 A. Zagdoun, G. Casano, O. Ouari, G. Lapadula, A. J. Rossini, M. Lelli, M. Baffert, D. Gajan, L. Veyre, W. E. Maas, M. Rosay, R. T. Weber, C. Thieuleux, C. Coperet, A. Lesage, P. Tordo and L. Emsley, *J. Am. Chem. Soc.*, 2012, **134**, 2284.
- 14 M. Tseitlin, J. R. Biller, H. Elajaili, V. V. Kramtsov, I. Dhimitruka, G. R. Eaton and S. S. Eaton, *J. Magn. Reson.*, 2014, **245**, 150.

15 B. Epel, G. Redler, V. M. Tormyshev and H. J. Halpern, Towards Human Oxygen Images with Electron Paramagnetic Resonance Imaging, *Oxygen Transport to Tissue XXXVII, V.876 of the series Advances in Experimental Medicine and Biology, Part VII*, 2015, p. 363.

16 O. Lafon, M. Rosay, F. Aussenac, X. Lu, J. Trébosc, O. Cristini, C. Kinowski, N. Touati, H. Vezin and J.-P. Amoureux, *Angew. Chem., Int. Ed.*, 2011, **50**, 8367.

17 G. Audran, P. Brémond and S. R. A. Marque, *Chem. Commun.*, 2014, **50**(59), 7921.

18 *Nitroxide Mediated Polymerization: From Fundamentals to Applications in Materials Science*, ed. D. Gigmes, Series: RSC Polymer Chemistry Series, 2015.

19 C. Yuan, M. Z. Rong, M. Q. Zhang and Z. P. Zhang, *Chem. Mater.*, 2011, **23**, 5076.

20 Z. P. Zhang, M. Z. Rong, M. Q. Zhang and C. Yuan, *Polym. Chem.*, 2013, **4**, 4648.

21 M. Becker, L. D. Cola and A. Studer, *Chem. Commun.*, 2011, **47**, 3392.

22 M. Becker, L. De Cola and A. Studer, *J. Mater. Chem. C*, 2013, **1**, 3287.

23 R. K. Roy, A. Meszynska, C. E. Laure, L. Charles, C. Verchin and J.-F. C. O. Lutz, *Nat. Commun.*, 2015, **6**, 1.

24 L. Charles, C. Laure, J.-F. Lutz and R. K. Roy, *Macromolecules*, 2015, **48**, 4319.

25 G. Audran, P. Brémond, J.-M. Franconi, S. R. A. Marque, P. Massot, P. Mellet, E. Parzy and E. Thiaudiere, *Org. Biomol. Chem.*, 2014, **12**, 719.

26 (a) Y. Liu, F. A. Villamena and J. L. Zweier, *Chem. Commun.*, 2008, 4336; (b) Y. Song, Y. Liu, C. Hemann, F. A. Villamena and J. L. Zweier, *J. Org. Chem.*, 2013, **78**, 1371.

27 S. Marque, C. Le Mercier, P. Tordo and H. Fischer, *Macromolecules*, 2000, **33**(12), 4403.

28 D. Bertin, D. Gigmes, S. R. A. Marque and P. Tordo, *Chem. Soc. Rev.*, 2011, **40**, 2189.

29 S. Stoll and A. Schweiger, *J. Magn. Reson.*, 2006, **178**, 42.

30 M. M. Goerger and B. S. Hudson, *J. Org. Chem.*, 1988, **53**, 3148.

31 S. Acerbis, D. Bertin, B. Boutevin and D. Gigmes, *Helv. Chim. Acta*, 2006, **89**, 2119.

32 G. Audran, P. Brémond, J.-P. Joly, S. R. A. Marque and T. Yamasaki, *Org. Biomol. Chem.*, 2016, **14**, 3574.

33 K. Matyjaszewski, B. E. Woodworth, X. Zhang, S. G. Gaynor and Z. Metzner, *Macromolecules*, 1998, **31**, 5955.

34 R. Nicolaï and K. Matyjaszewski, *Macromolecules*, 2011, **44**, 240.

35 O. Y. Rogozhnikova, V. G. Vasiliev, T. I. Troitskaya, D. V. Trukhin, T. V. Mikhalina, H. J. Halpern and V. M. Tormyshev, *Eur. J. Org. Chem.*, 2013, 3347.

36 This procedure is a modified version of D. Trukhin, O. Rogozhnikova, T. Troitskaya, V. Vasiliev, M. Bowman and V. Tormyshev, *Synlett*, 2016, 893.

37 S. Marque, *J. Org. Chem.*, 2003, **68**(20), 7582.

38 T. Fujita, C. Takayama and M. Nakajima, *J. Org. Chem.*, 1973, **38**, 1623.

39 H. Fischer, A. Kramer, S. R. A. Marque and P. Nesvadba, *Macromolecules*, 2005, **38**, 9974.

40 M. Charton, *Prog. Phys. Org. Chem.*, 1981, **13**, 119.

41 M. Charton, *Adv. Mol. Struct. Res.*, 1999, **5**, 25.

42 D. Bertin, D. Gigmes, S. R. A. Marque, S. Milardo, J. Peri and P. Tordo, *Collect. Czech. Chem. Commun.*, 2004, **69**, 2223.

43 G. Audran, P. Brémond, S. R. A. Marque and T. Yamasaki, *J. Org. Chem.*, 2016, **81**, 1981.

44 E. Beaudoin, D. Bertin, D. Gigmes, S. R. A. Marque, D. Siri and P. Tordo, *Eur. J. Org. Chem.*, 2006, 1755.

45 P. Brémond and S. R. A. Marque, *Chem. Commun.*, 2011, **47**, 4291.

46 P. Brémond, A. Koïta, S. R. A. Marque, V. Pesce, V. Roubaud and D. Siri, *Org. Lett.*, 2012, **14**, 358.

47 S. R. A. Marque and D. Siri, *Macromolecules*, 2009, **42**(4), 1404.

48 C. Chachaty, W. Huang, L. Marx, B. Charleux and A. Rassat, *Polymer*, 2003, **44**, 397.

49 Y. Liu, F. A. Villamena, A. Rockenbauer, Y. Song and J. L. Zweier, *J. Am. Chem. Soc.*, 2013, **135**, 2350.

50 *Alkoxy, carbonyloxy, phenoxy, and related radicals, Radical reaction rates in liquids*, ed. H. Fischer, Landolt-Börnstein Springer Verlag, Berlin Heidelberg, 1997, group II, vol. 18, suppl. vol. II/13, subvolume A.

51 C. Decroos, Y. Li, G. Bertho, Y. Frapart, D. Mansuy and J.-L. Boucher, *Chem. Commun.*, 2009, 1416.

52 C. Decroos, Y. Li, A. Soltani, Y. Frapart, D. Mansuy and J.-L. Boucher, *Arch. Biochem. Biophys.*, 2010, **502**, 74.

53 C. Decroos, T. Prangé, D. Mansuy, J.-L. Boucher and Y. Li, *Chem. Commun.*, 2011, **47**, 4805.

54 K. U. Ingold, *Acc. Chem. Res.*, 1969, **2**, 1.

55 J. Howard, *Alkoxy, carbonyloxy, phenoxy, and related radicals, Radical reaction rates in liquids*, ed. H. Fischer, Landolt-Börnstein Springer Verlag, Berlin Heidelberg, 1997, group II, vol. 18, suppl. vol. II/13, subvolume D2.

56 P. Brémond, K. Kabytaev and S. R. A. Marque, *Tetrahedron Lett.*, 2012, **53**, 4543.

57 J. Lusztyk, *Alkoxy, carbonyloxy, phenoxy, and related radicals, Radical reaction rates in liquids*, ed. H. Fischer, Landolt-Börnstein Springer Verlag, Berlin Heidelberg, 1997, group II, vol. 18, suppl. vol. II/13, subvolume A.

58 D. Gigmes, D. Bertin, C. Lefay and Y. Guillaneuf, *Macromol. Theory Simul.*, 2009, **18**, 402.

59 D. Gigmes and S. R. A. Marque, *Encyclopedia of Radicals in Chemistry, Biology, and Materials*, ed. C. Chatgilialoglu and A. Studer, Wiley, Chichester, U.K., 2012, p. 1813.

60 J. Nicolas, Y. Guillaneuf, C. Lefay, D. Bertin, D. Gigmes and B. Charleux, *Prog. Polym. Sci.*, 2013, **38**, 63.

